Received: 12 November 2018 | Revised: 18 February 2019 | Accepted: 7 April 2019

DOI: 10.4218/etrij.2018-0614

ORIGINAL ARTICLE

ETRI Journal WILEY

Robust range-only beacon mapping in multipath environments

Byungjae Park[1] | **Sejin Lee**[2]

[1]Intelligence and Robot Research Session, Electronics and Telecommunications Research Institute, Daejeon, Rep. of Korea

[2]Department of Mechanical and Automotive Engineering, Kongju National University, Cheonan, Rep. of Korea

Correspondence
Sejin Lee, Department of Mechanical and Automotive Engineering, Kongju National University, Cheonan, Rep. of Korea.
Email: sejiny3@kongju.ac.kr

Funding information
Ministry of Science, ICT and Future Planning, Grant/Award Number: 2017-0-00067 and 2017-0-00306

This study proposes a robust range-only beacon mapping method for registering the locations of range-only beacons automatically. The proposed method deals with the multipath propagation of signals from range-only beacons using the range-only measurement association (RoMA) and an unscented Kalman filter (UKF). The RoMA initially predicts the candidate positions of a range-only beacon. The location of the range-only beacon is then updated using the UKF. With the proposed method, the locations of range-only beacons are accurately estimated in a multipath environment. The proposed method also provides the location uncertainty of each range-only beacon. Simulation results using the model for multipath propagation and experimental results in a real indoor environment verify the performance of the proposed method.

KEYWORDS
location-based service, mapping, multipath environment, range-only sensor, ultra-wideband

1 | INTRODUCTION

Precise localization of a mobile node is essential for various location-based services [1].

A GPS-based localization method is commonly used to estimate the position of a mobile node in an outdoor environment because of the following advantages [2,3]: (i) it requires only a small receiver unit to acquire signals from GPS satellites and (ii) a map is not required. However, this method cannot be used to estimate the position of a mobile node in an indoor environment because signals from GPS satellites are blocked by various structures such as walls or buildings [4]. If a receiver unit cannot acquire signals from a sufficient number of GPS satellites, this method cannot estimate the position of a mobile node accurately or may fail to estimate the position entirely. Range-only beacon-based localization methods have been proposed to estimate the position of a mobile node in a GPS-denied environment [5]. These methods estimate the position of a mobile node by associating multiple range-only measurements between a mobile node and range-only beacons. Triangulation is a well-known technique used to estimate the position of a mobile node. It uses the time-of-arrival (ToA) or time-difference-of-arrival (TODA) to associate multiple range-only measurements [1,6,7]. Various devices such as RFID, WiFi, Bluetooth, and ultra-wideband (UWB) communications devices can be used as a range-only beacon for a triangulation approach. Among them, UWB communication devices are more commonly used than other devices [8,9] because they are cost-effective, compact, and provide accurate distance measurements. With a UWB communication, the distance between a sender and receiver is calculated using the difference between the sending and receiving times of a very short pulse. A Ubisense sensor system is a well-known indoor localization solution that uses UWB communication devices [10]. The system consists of several fixed UWB communication devices, an active mobile tag, and software. The distance between each fixed UWB communication device and the active mobile tag is computed using a transmitted signal from the active mobile tag. The position of the active mobile tag is estimated through software using the TODA and angle-of-arrival data fusion methods. The system estimates the position of the active mobile tag with submeter accuracy and can cover an area as large as 400 m^2 with four fixed UWB communication devices.

Although range-only beacon-based localization methods using UWB communication devices can estimate the position of a mobile node in a GPS-denied environment accurately, they have certain limitations. To estimate the position of a mobile node using range-only beacons accurately, an accurate map of range-only beacons must be available. If the locations of some range-only beacons are incorrectly mapped, the estimation of the position of a mobile node will be inaccurate. In a small environment, the locations of range-only beacons can be registered manually. However, manual registration cannot be utilized in a large environment.

An autonomous registration is required to build a map of range-only beacons in a large environment. Unfortunately, autonomous registration is a challenging issue because of the properties of a range-only beacon. A range-only beacon does not provide a bearing measurement. Moreover, a range measurement provided by a range-only beacon contains extensive noise when the line-of-sight (LOS) between a range-only beacon and a mobile node does not exist. The LOS should be required to measure accurately the distance between a range-only beacon and a mobile node. If no LOS exists, multipath propagation will occur [11,12]. The distance is inaccurately measured because the signal from a range-only beacon is indirectly received or delayed. The distance measured from an indirectly received or delayed signal has large uncertainty.

To overcome this problem, various autonomous registration methods have been proposed. Most of them can be classified into two approaches. The first approach uses intercommunication between range-only beacons to estimate the beacon locations. The ad-hoc localization and direct position estimation methods compute the location of each range-only beacon by recursively measuring the distances from the neighboring range-only beacons [13,14]. Shell sweeps and component-based methods have been proposed to estimate the locations of range-only beacons using their graphical structures, which represent the intercommunication connectivity of range-only beacons [15,16]. These methods build graphical structures of the range-only beacons and then estimate the locations of the beacons by partitioning the graphical structures and merging the graphical substructures. An intercommunication-based approach is used to estimate the locations of range-only beacons without using any external information. However, this approach has certain limitations. If the connectivity of the range-only beacons is sparse, their locations cannot be accurately estimated. In addition, this approach cannot deal with multipath propagation.

The second approach uses various probabilistic estimation techniques in robotics. With this approach, a mobile node acquires measurements from range-only beacons while moving within an environment, and the locations of range-only beacons are then estimated using the acquired measurements and odometry information of a mobile node [17]. Various methods using this approach focus on the bearing ambiguities of range-only measurements. Gaussian mixture model-based mapping methods have been proposed to estimate the locations of range-only beacons [18,19]. These methods model the bearing uncertainties of range-only measurements using a mixture of Gaussians. The voting-based method has been proposed to estimate the locations of range-only beacons [20]. This method uses a 2D grid map to accumulate the possible location of each range-only beacon. Two point intersections of two range-only measurements, which are acquired in two positions, are estimated, and two votes are then assigned to the two corresponding grid cells within the 2D grid map. Although the probabilistic estimation-based approach can reduce the bearing ambiguities of range-only measurements, this approach is not sufficiently robust to deal with large measurement noises caused by multipath propagation.

To resolve the bearing ambiguities and large measurement noises of range-only measurements, we propose a robust range-only beacon mapping method to estimate the locations of range-only beacons on a map. The proposed method estimates the locations of range-only beacons using the following procedure: (i) the location of each range-only beacon is initially predicted by range-only measurement association (RoMA) and random sample consensus (RANSAC), and (ii) the location is then updated using an unscented Kalman filter (UKF)[21,22] . With the proposed method, the locations of range-only beacons are mapped accurately in multipath environments.

The remainder of this paper is organized as follows. The RoMA and feature prediction using the RoMA and RANSAC are described in Section 2. The feature update using the UKF is presented in Section 3. The simulation and experimental results are presented in Sections 4 and 5, respectively. Some concluding remarks are given in Section 6.

2 | FEATURE PREDICTION

2.1 | Range-only Measurement Association

RoMA, which is motivated by the footprint association of sonar sensor data [23], computes two candidate locations of a range-only beacon by combining two range-only measurements acquired at two positions (Figure 1). The two circle labeled z_i and z_j are range-only measurements acquired at x_i and x_j, respectively. The candidate locations of the kth range-only beacon can be computed using the RoMA:

$$f_k^s(x_i, z_i, x_j, z_j) = R(x_i, x_j) \begin{bmatrix} z_i \times \frac{z_i^2 - z_j^2 + d(x_i, x_j)}{2d(x_i, x_j)} \\ sz_i \times \left(1 - \left(\frac{z_i^2 - z_j^2 + d(x_i, x_j)}{2d(x_i, x_j)}\right)^2\right)^{\frac{1}{2}} \end{bmatrix} + t(x_i, x_j) \quad \left(s = \pm 1, d(x_i, x_j) > D_{\min}\right), \tag{1}$$

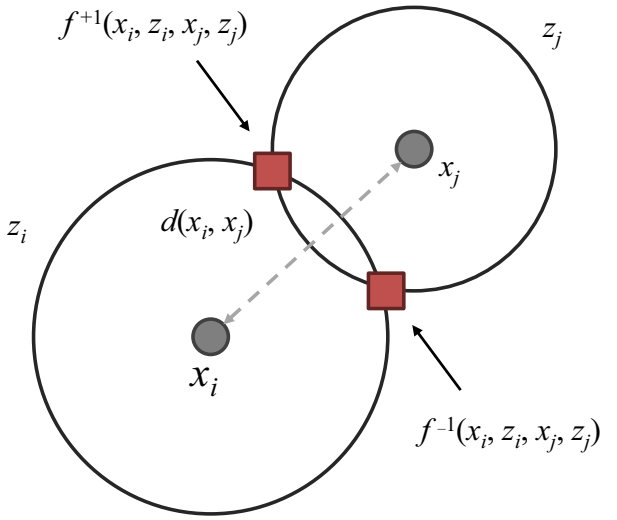

FIGURE 1 RoMA computes two candidate locations of a range-only beacon by combining two range-only measurements. The black circles and dots represent range-only measurements and the positions of a mobile device, respectively. The red boxes represent the candidate locations of a range-only beacon

where $d(x_i, x_j)$ is the distance between x_i and x_j, and $R(x_i, x_j)$ and $t(x_i, x_j)$ are the rotation matrix and translation vector between x_i and x_j, respectively. $f_k^{-1}(x_i, z_i, x_j, z_j)$ is the first candidate location of the kth range-only beacon, and $f_k^{+1}(x_i, z_i, x_j, z_j)$ is the second candidate location of the kth range-only beacon. $D_{\min}$ is the minimum distance between x_i and x_j. $D_{\min}$ was set as 0.1 m in both the simulations and experiment.

The mean and covariance of each candidate location of a range-only beacon can be estimated by applying the unscented transform to the RoMA. If the kth range-only beacon is observed at x_i and x_j, the estimated mean and covariance of the location of the kth range-only beacon is computed using the sigma points from the augmented range-only measurement [21,22]:

$$z' = \begin{bmatrix} x_i \\ z_i \\ \mathrm{x}_j \\ z_j \end{bmatrix}, \quad R' = \begin{bmatrix} P_i & & & \\ & R & & \\ & & P_j & \\ & & & R \end{bmatrix}, \tag{2}$$

where z' and R' are the mean and covariance of the augmented range-only measurement, respectively, P_i and P_j are the covariances of x_i and x_j, respectively, and R is the measurement noise of a range-only beacon. Note that the augmented state contains the mobile node positions of two range-only measurements. Through augmentation, their uncertainties, such as odometry errors, are also considered in estimating the mean and covariance of the location of a range-only beacon. A symmetric set of sigma points is computed as follows:

$$\begin{aligned} \chi_{\bar{z}}'^{[0]} &= z', \\ \chi_{\bar{z}}'^{[i]} &= z' + \left(\sqrt{(L+\lambda)R'}\right)_i \qquad i = 1, \ldots, L, \\ \chi_{\bar{z}}'^{[i]} &= z' - \left(\sqrt{(L+\lambda)R'}\right)_i \qquad i = L+1, \ldots, 2L, \end{aligned} \tag{3}$$

where L is the length of the augmented range-only measurement, n is the dimension of the augmented range-only measurement $n = 6$, and λ is computed as $\lambda = \alpha^2(L + \kappa) - L$ and $\alpha(0 < \alpha < 1)$ [21]. The computed sigma points are transformed based on the function of the RoMA as:

$$\bar{\chi}_{\bar{z}}^{[i]} = f^s(\chi_{\bar{z}}'^{[i]}). \tag{4}$$

The estimated mean and covariance of the candidate location of a range-only beacon are computed using the weighted sum of the transformed sigma points:

$$\mu_k = \sum_{i=0}^{2L} w_{\mathrm{g}}^{[i]} \bar{\chi}_{\bar{z}}^{[i]}, \tag{5}$$

$$\Sigma_k = \sum_{i=0}^{2L} w_c^{[i]} \left(\bar{\chi}_{\bar{z}}^{[i]} - \mu\right) \times \left(\bar{\chi}_{\bar{z}}^{[i]} - \mu\right)^{\mathrm{T}}. \tag{6}$$

Here, weight $w_{\mathrm{g}}^{[i]}$ is used to compute the estimated mean of the location of a range-only beacon and weight $w_{\mathrm{c}}^{[i]}$ is used to recover the estimated covariance of this location.

$$\begin{aligned} w_{\mathrm{g}}^{[0]} &= \frac{\lambda}{L+\lambda}, \\ w_{\mathrm{c}}^{[0]} &= \frac{\lambda}{L+\lambda} + \left(1 - \alpha^2 + \beta\right), \\ w_{\mathrm{g}}^{[i]} &= w_c^{[i]} = \frac{\lambda}{2(L+\lambda)} \quad i = 1, \ldots, 2L, \end{aligned} \tag{7}$$

where β is the parameter incorporating the knowledge of the higher order moments of the posterior distribution. For the Gaussian prior, the optimal choice is $\beta = 2$ [21].

2.2 | Feature selection and outlier removal

The proposed method uses RANSAC to determine the location of a range-only beacon among two candidate locations determined by the RoMA and to filter out incorrect range-only measurements affected by multipath propagation. The procedure using the RANSAC-based feature initialization is shown in Figure 2. To determine the inliers, an expected range-only measurement from a candidate location of a range-only beacon and an observed range-only measurement are compared. If the difference between the expected and observed range-only measurements is smaller than the given threshold, the observed range-only measurement is considered to be an inlier.

procedure FEATUREPREDICTION($X = \{x_1, \cdots\}, Z = \{z_1, \cdots\}$)
  $\mu_B \leftarrow [\,], \Sigma_B \leftarrow [\,]$
  $Z_B \leftarrow \emptyset$
  repeat
    $x_i, z_i, x_j, z_j \leftarrow$ `SelectRandomSubset`(X, Z)
    $\mu_H^{-1}, \Sigma_H^{-1}, \mu_H^{+1}, \Sigma_H^{+1} \leftarrow$ `ComputeRoMA`(x_i, z_i, x_j, z_j)
    $Z_H^{-1}, Z_H^{+1} \leftarrow$ `ComputeInliers`$(\mu_H^{-1}, \Sigma_H^{-1}, \mu_H^{+1}, \Sigma_H^{+1})$
    if $n(Z_H^{-1}) > n(Z_H^{+1})$ **then**
      $\mu_H \leftarrow \mu_H^{-1}, \Sigma_H \leftarrow \Sigma_H^{-1}$
      $Z_H \leftarrow Z_H^{-1}$
    else
      $\mu_H \leftarrow \mu_H^{+1}, \Sigma_H \leftarrow \Sigma_H^{+1}$
      $Z_H \leftarrow Z_H^{+1}$
    end if
    if $n(Z_B) < n(Z_H)$ **then**
      $\mu_B \leftarrow \mu_H, \Sigma_B \leftarrow \Sigma_H$
      $Z_B \leftarrow Z_H$
    end if
  until the best hypothesis is founded
  return μ_B, Σ_B, Z_B ▷ return mean, covariance, and inliers
end procedure

FIGURE 2 Feature prediction using RoMA and RANSAC

The location of a range-only beacon is sequentially updated using the inliers of range-only measurements determined through the RANSAC-based feature selection and outlier removal.

3 | FEATURE UPDATE

The UKF is applied to update the mean and covariance of the location of a range-only beacon [21,22]. In the UKF-based feature update, a mobile node position and its uncertainty are also augmented to compute the sigma points:

$$\mu'_{k,t-1} = \begin{bmatrix} \mu_{k,t-1} \\ x_p \\ z_p \end{bmatrix}, \quad \Sigma'_{k,t-1} = \begin{bmatrix} \Sigma_{k,t-1} & & \\ & P_p & \\ & & R \end{bmatrix}, \tag{8}$$

where x_p and P_p are the mean and covariance of the mobile node position, respectively. z_p is the range-only measurement at x_p. The range-only measurement noise covariance R is also augmented to consider the measurement noise. The sigma points are computed using the augmented mean and covariance of the location of a range-only beacon:

$$\begin{aligned} \chi'^{[0]}_{\mu'_{k,t-1}} &= \mu'_{k,t-1}, \\ \chi'^{[i]}_{\mu'_{k,t-1}} &= \mu'_{k,t-1} + \left(\sqrt{(k+\lambda)\Sigma'_{k,t-1}}\right)_i \quad i = 1, \ldots, M, \\ \chi'^{[i]}_{\mu'_{k,t-1}} &= \mu'_{k,t-1} - \left(\sqrt{(k+\lambda)\Sigma'_{k,t-1}}\right)_i \quad i = n+1, \ldots, 2M, \end{aligned} \tag{9}$$

where $\mu'_{k,t-1}$ and $\Sigma'_{k,t-1}$ are the augmented mean and covariance of the location of a range-only beacon, respectively. The value of M is the dimension of a feature state. In this case, $M = 4$ and $\lambda = \alpha^2(L + k) - M$. Each sigma point $\chi'^{[i]}_{\mu'_{k,t-1}}$ contains the location of a range-only beacon, mobile node position, and measurement noise:

$$\chi'^{[i]}_{\mu'_{k,t-1}} = \begin{bmatrix} \chi^{[i]}_{\mu'_{k,t-1}} \\ \chi^{x[i]}_{\mu'_{k,t-1}} \\ \chi^{z[i]}_{\mu'_{k,t-1}} \end{bmatrix}. \tag{10}$$

The observation model h is characterized by a nonlinear function and the sigma points are transformed through the observation model:

$$\bar{z}^{[i]} = h\left(\chi'^{[i]}_{\mu'_{k,t-1}}\right) = \left\| \chi^{[i]}_{\mu'_{k,t-1}} - \chi^{x[i]}_{\mu'_{k,t-1}} \right\|. \tag{11}$$

The predicted range-only measurement $\hat{z}_p$ at x_p and its innovation covariance $\bar{S}_p$ are defined as follows:

$$\hat{z}_p = \sum_{i=0}^{2M} w_g^{[i]} \bar{z}^{[i]}, \tag{12}$$

$$\bar{S}_k = \sum_{i=0}^{2M} w_c^{[i]} \left(\bar{z}^{[i]} - \hat{z}_p\right) \times \left(\bar{z}^{[i]} - \hat{z}_p\right)^{\mathrm{T}}, \tag{13}$$

Here, $\bar{\Sigma}_p$ is the cross-covariance between the state of a range-only beacon and range-only measurement, and is calculated as follows:

$$\bar{\Sigma}_p = \sum_{i=0}^{2M} w_c^{[i]} \left(\chi^{[i]}_{\mu'_{k,t-1}} - \mu_{k,t-1}\right) \times \left(\bar{z}^{[i]} - \hat{z}_p\right)^{\mathrm{T}} \tag{14}$$

The Kalman gain is computed using the cross-covariance:

$$\bar{K}_p = \bar{\Sigma}_p \left(\bar{S}_p\right)^{-1}. \tag{15}$$

Finally, the mean and covariance of the n range-only beacon are updated as follows:

$$\mu_{k,t} = \mu_{k,t-1} + \bar{K}_p \left(z_p - \hat{z}_p\right), \tag{16}$$

$$\Sigma_{k,t} = \Sigma_{k,t-1} - \bar{K}_p \bar{S}_p \bar{K}_p^{\mathrm{T}}. \tag{17}$$

To update the mean and covariance of the location of a range-only beacon, the Cholesky factorization is applied to guarantee the numerical stability.

4 | SIMULATION RESULTS

Simulations were conducted to verify that the proposed method robustly estimates the locations of range-only sensors in a multipath environment. Simulations were run on a laptop using Python and Numpy. The {TOA data fusion} was

used as a baseline [6]. The multipath propagation model of a UWB communication device was adopted to conduct more realistic simulations [24]. Two scenarios were used for the simulations: (i) a rectangular environment and (ii) an indoor environment.

4.1 | Multipath propagation model

The multipath propagation model considers various characteristics of UWB communication devices and the presence or absence of a direct path (DP) under LOS or non-LOS (NLOS) conditions between a range-only beacon and a mobile node.

A DP always exists under LOS conditions. However, a DP may not exist under NLOS conditions. If a DP exists under NLOS conditions, the dominant source of a range-only measurement error is the propagation delay. This occurs when the speed of the transmission of a signal is slowed through an object. The propagation delay adds a small positive bias to a range-only measurement. If a DP does not exist under NLOS conditions when objects such as walls, doors, or furniture block a signal between a range-only beacon and a mobile node, a mobile node will receive indirect signals reflected by the surfaces of other objects. Their paths are different from a blocked direct path between a range-only beacon and a mobile node. The distances of the indirect paths are longer than the blocked direct signal path. Therefore, a large-positive bias is added to a range-only measurement when a DP does not exist under NLOS conditions.

The normalized measurement error is defined as follows [11]:

$$\psi = \frac{\varepsilon}{z_{GT}} = \frac{z - z_{GT}}{z_{GT}}, \tag{18}$$

where z and z_{GT} are the observed and ground truth measurements, respectively. The normalized measurement error can be modeled by considering the presence or absence of the DP and LOS as follows [11]:

$$\psi = \psi_m + G(\psi_{pd} + B\psi_b), \tag{19}$$

$$G = \begin{cases} 0 & \text{LOS conditions} \\ 1 & \text{NLOS conditions,} \end{cases}$$

$$B = \begin{cases} 0 & \text{DP exists} \\ 1 & \text{DP does not exist,} \end{cases}$$

where ψ_w is a zero-mean white noise that always exists under both LOS and NLOS conditions, ψ_{pd} is the normalized propagation delay induced error under NLOS conditions ($G = 1$), and ψ_b is the blockage error. The blockage error occurs ($B = 1$) when the DP does not exist. The probability of the occurrence of a blockage error depends on the bandwidth of a range-only beacon and the configuration of the indoor environment.

Based on the normalized measurement error, the multipath propagation model can be defined using the following equation [11]:

$$f(\psi|G,B) = \begin{cases} \frac{1}{\sqrt{2\pi\sigma_m^2}} \exp\left[-\frac{(\psi-\mu_m)^2}{2\sigma_m^2}\right] & G=0 \\ \frac{1}{\sqrt{2\pi\sigma_{pd}^2}} \exp\left[-\frac{(\psi-\mu_{pd})^2}{2\sigma_{pd}^2}\right] & G=1, B=0 \\ \frac{1}{\psi\sqrt{2\pi\sigma_b^2}} \exp\left[-\frac{(\ln\psi-\mu_b)^2}{2\sigma_b^2}\right] & G=1, B=1 \end{cases}. \tag{20}$$

Note that the multipath propagation model when the blockage error occurs under NLOS conditions has a log-normal distribution. In this case, the normalized measurement noise is larger than that of the other cases. The parameters used to compute the multipath propagation model are shown in Table 1 [11].

4.2 | Rectangular environment scenario

In this scenario, the locations of 16 range-only beacons were estimated using range-only measurements acquired at 49 positions in a simple rectangular environment. The detailed parameters are listed in Table 2.

The probability of being under NLOS conditions $P(G = 1)$ was varied from 0.01 to 0.50. Figure 3 shows the results of the simulations. Figures 3A and 3B show the mean mapping errors of the proposed method and

TABLE 1 Multipath propagation model parameters

	Parameters	Value
	500 MHz	3 GHz
(μ_m, σ_m)	(0, 0.028)	(0, 0.006)
(μ_{pd}, σ_{pd})	(0.058, 0.028)	(0.03, 0.01)
(μ_b, σ_b)	(−1.68, 0.88)	(−1.90, 1.13)

TABLE 2 Rectangular environment scenario parameters

	Parameters	Value
UWB	Bandwidth	500 MHz, 3 GHz
	Environment width	40 m
	Environment height	40 m
	Maximum measurement range	25 m
	$P(G = 1)$	0.00–0.50
	$P(G = 1, B = 1)$	0.80
Mobile node	Odometry error	0.20 m

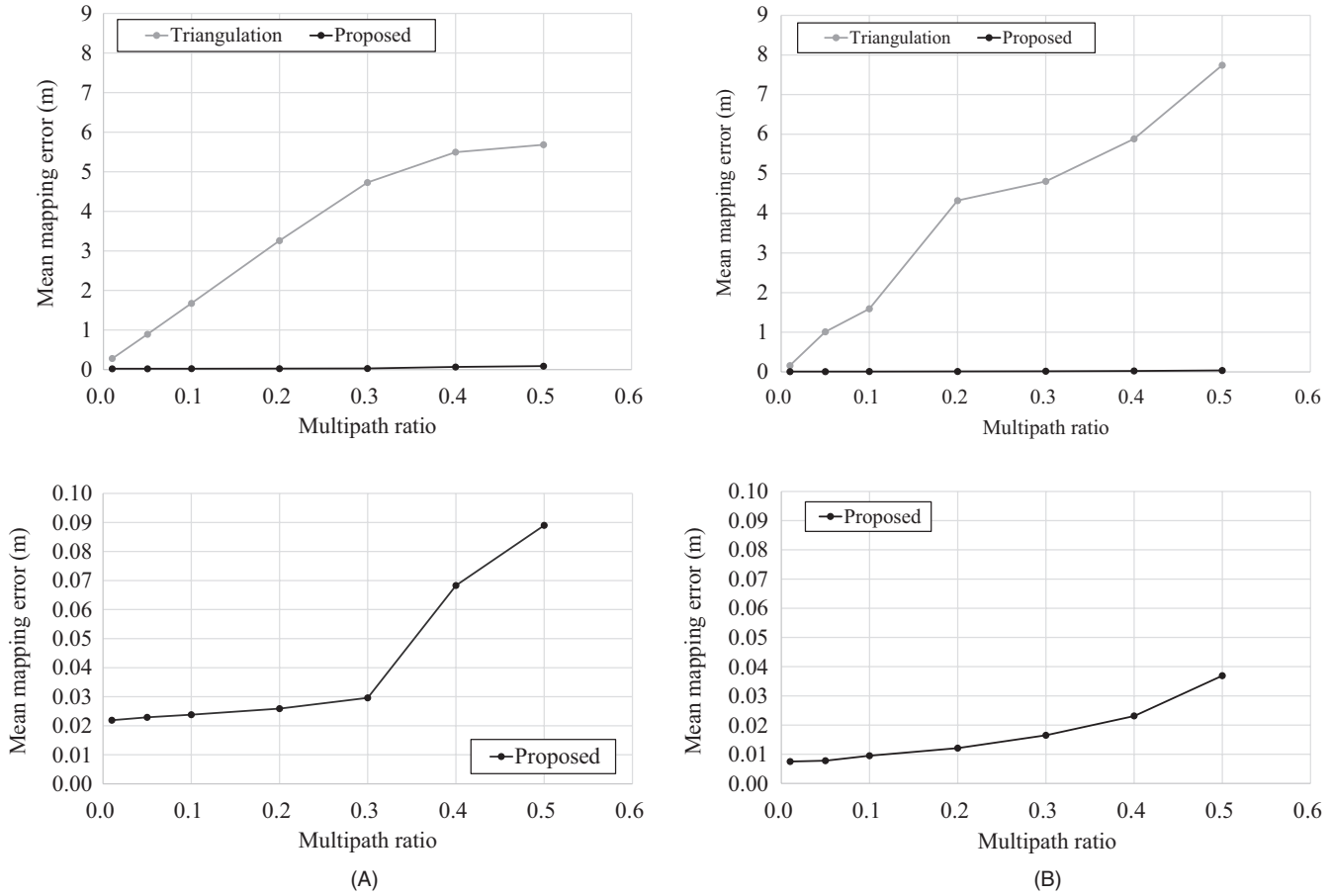

FIGURE 3 Simulation results when varying the probabilities of being under NLOS conditions (100 runs): (A) 500 MHz bandwidth, and (B) 3 GHz bandwidth

TOA data fusion using 500 MHz and 3 GHz range-only beacons, respectively. The upper sections of these figures show the mean mapping errors of the proposed method and TOA data fusion. The mean mapping errors of the TOA data fusion increased rapidly as the probability of being under NLOS conditions increased because a least squares regression is highly sensitive to outliers. When 5% of the range-only measurements were affected by the propagation delays and blockages, the mean mapping errors increased significantly (500 MHz: 147%, 3 GHz: 796%). However, the mean mapping errors of the proposed method increased only slightly as the probability of being under NLOS conditions increased. The lower sections of these figures illustrate a magnified view of the mean mapping errors of the proposed method. The proposed method estimated the locations of the range-only beacons much more accurately than did the TOA data fusion even though a considerable portion of range-only measurements were affected by the propagation delays and blockage errors. This is because the proposed method was able to filter out unreliable range-only measurements using RANSAC.

Figure 4 shows the estimated locations of range-only beacons using the TOA data fusion and proposed method. The probability of being under NLOS conditions $P(G = 1)$ was set to 0.30. The red and black dots represent the true and estimated locations of range-only beacons, respectively, and the gray dots represent the positions where a mobile node acquires range-only measurements from range-only beacons. The estimated locations of 500 MHz and 3 GHz range-only beacons using the TOA data fusion are shown in Figures 4A and 4C respectively. The TOA data fusion estimated the locations of range-only beacons inaccurately. In particular, the mapping errors of some range-only beacons were extremely large. Specifically, their mapping errors were larger than several meters. In addition, the locations of range-only beacons were accurately estimated using the proposed method. The estimated locations of 500 MHz and 3 GHz range-only beacons using the proposed method are shown in Figures 4B and 4D respectively. The average mapping errors measured using the proposed method were smaller than 0.1 m (500 MHz: 0.0273 m, 3 GHz: 0.0233 m). It is also notable that the proposed method could estimate the locations of range-only beacons as well as their uncertainties because the proposed method uses a probabilistic approach. In these figures, the uncertainties of the estimated locations of range-only

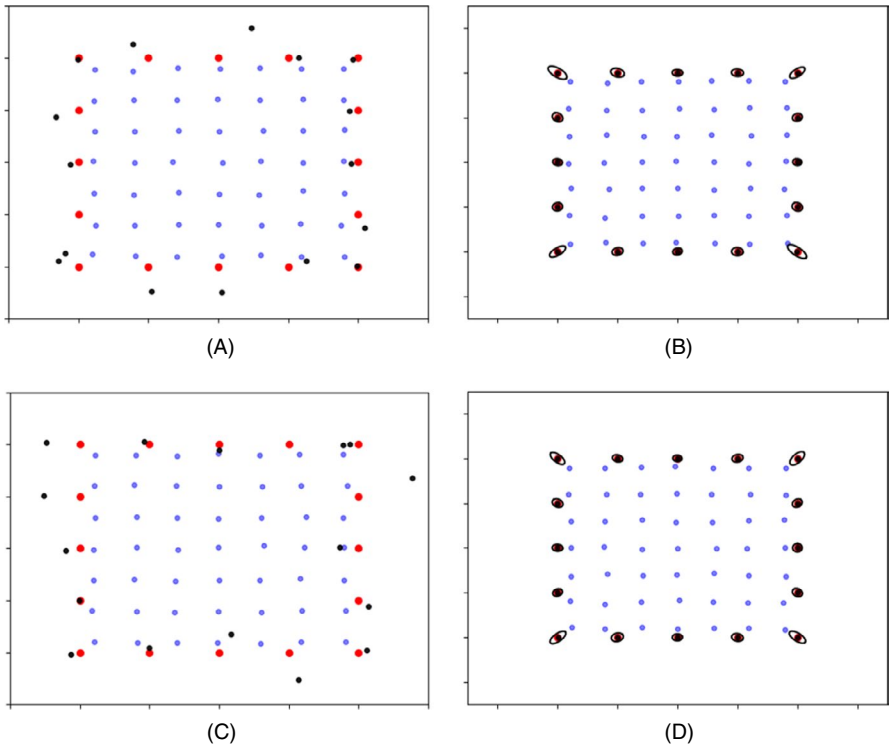

FIGURE 4 Range-only mapping simulation results using the TOA data fusion and proposed method under NLOS conditions. Blue dots represent the positions where a mobile node acquires range-only measurements from range-only beacons. Red dots represent the ground truth locations of range-only beacons. Black dots and ellipses represent the estimated locations of range-only beacons and their uncertainties (3σ). The size of each ellipse is magnified four times. (A) TOA data fusion, 500 MHz bandwidth, (B) proposed method, 500 MHz bandwidth, (C) TOA data fusion, 3 GHz bandwidth, and (D) proposed method, 3 GHz bandwidth

beacons are also represented by the black ellipses. The size of each ellipse is magnified four times for better visualization. The uncertainties of the locations of range-only beacons can be used when the position of a mobile node is tracked using range-only beacons.

4.3 | Indoor environment scenario

In this scenario, the locations of range-only beacons were estimated in an indoor environment. The indoor environment had six 3 GHz range-only beacons. The parameters for this scenario are listed in Table 3. To simulate range-only measurements under LOS and NLOS conditions, we used a map of the environment. When no obstacles were present between the positions of a mobile node and range-only beacon, a range-only measurement was not affected by the propagation delay and blockage error $P(G = 0)$. Otherwise, a range-only measurement was affected by the propagation delay and blockage error. The range-only measurements affected by the propagation delays and blockage errors were modeled based on the given probabilities of being under NLOS conditions $P(G = 1)$ and of the occurrence of blockage $P(G = 1, B = 1)$. A considerable number of range-only measurements were affected by the propagation delays and blockage errors. Approximately 41% (Table 3) of the range-only measurements were affected by the propagation delays and blockage errors in this scenario.

TABLE 3 Indoor environment scenario parameters

	Parameters	Value
UWB	Bandwidth	3 GHz
	Environment width	20 m
	Environment height	20 m
	Maximum measurement range	25 m
	$P(G = 1)$	0.41
	$P(G = 1, B = 1)$	0.80
Mobile node	Odometry error	0.20 m

Table 4 shows mapping results using the TOA data fusion and proposed method. The proposed method estimated the locations of range-only beacons in dense multipath environments much more accurately than did the TOA data fusion.

Figure 5 shows range-only mapping results using the TOA data fusion and proposed method in the indoor environment under NLOS conditions. The locations of range-only beacons were very poorly mapped using the TOA data fusion. Every range-only beacon was mapped outside of the environment (Figure 5). This was because of the propagation delays or blockage errors. If a range-only measurement was affected by the propagation delay or blockage error, the measured distance between a mobile node and range-only beacon tended to be longer than the ground truth distance. The average mapping error

TABLE 4 Simulation results in the indoor environment (100 runs)

	Mean	Std.
TOA data fusion (m)	7.3690	5.8202
Proposed (m)	0.1190	0.0260

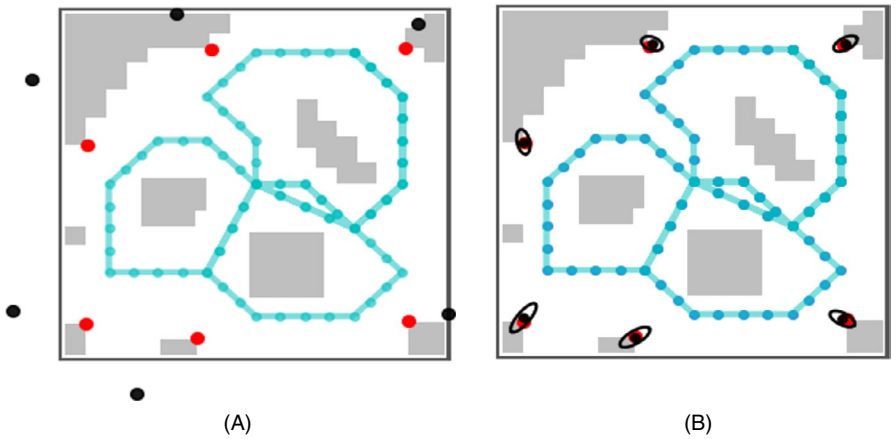

FIGURE 5 Range-only mapping simulation results using the TOA data fusion method and proposed method in the indoor environment and under NLOS conditions. Blue dots represent the positions where a mobile node acquires range-only measurements from range-only beacons, and blue lines represent the trajectory of a mobile node. Red dots represent the ground truth locations of range-only beacons. Black dots and ellipses represent the estimated locations of range-only beacons and their uncertainties (3σ). The size of each ellipse is magnified three times. Range-only mapping result using the (A) TOA data fusion and (B) proposed method

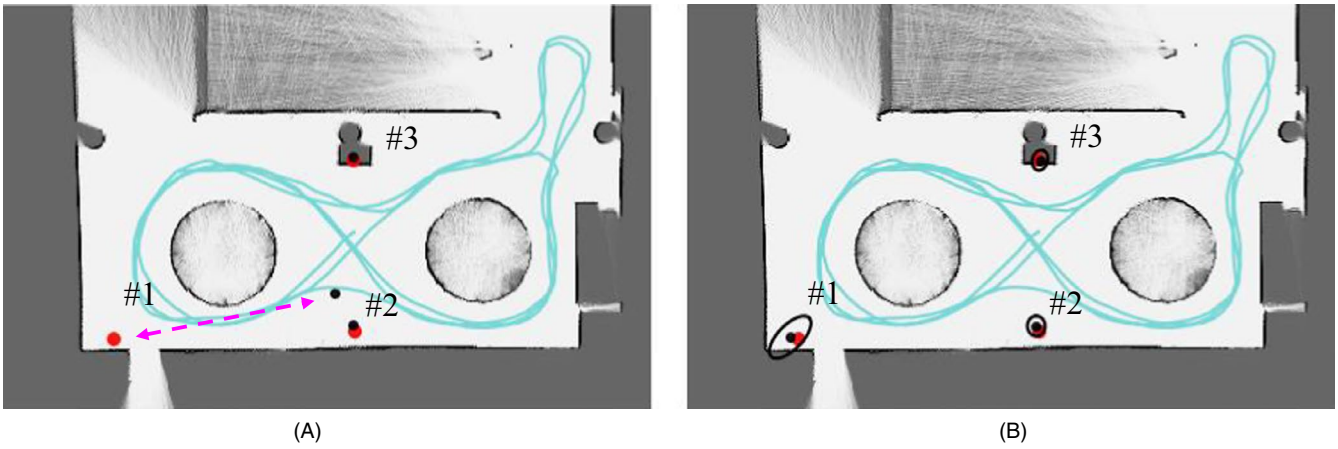

FIGURE 6 Experimental range-only mapping results using the TOA-based data fusion and proposed method in a real indoor environment. Blue lines represent the trajectory of the mobile robot computed by the ICP using one 2D LiDAR and several wheel encoders. Red dots represent the ground truth locations of the range-only beacons. Black dots and ellipses represent the estimated locations of range-only beacons and their uncertainties (3σ). The size of each ellipse is twice magnified. (A) Range-only mapping result using the TOA data fusion. The magenta dotted line represents the mapping error of the range-only beacon #1 estimated using the TOA data fusion. (B) Range-only mapping result using the proposed method

using the TOA data fusion was larger than several meters. In addition, the proposed method estimated more accurate locations of the range-only beacons.

5 | EXPERIMENTAL RESULTS

We conducted an experiment using a public dataset to verify the performance of the proposed method in a real indoor environment. The public dataset [24] was acquired using three 3-GHz range-only beacons and one Pioneer 3DX mobile robot, which had one 2D LiDAR and several wheel encoders. The positions of the mobile robot were computed using the iterative closest point (ICP) [25].

TABLE 5 Experimental results in the real indoor environment

	Beacon ID		
	#1	#2	#3
TOA data fusion (m)	6.1067	0.1587	0.0527
Proposed (m)	0.2124	0.1393	0.0764

TABLE 6 Measurement errors in the real indoor environment

	Beacon ID		
	#1	#2	#3
$\lvert z - z_{GT} \rvert$ (m)	2.9491	0.1116	0.0866

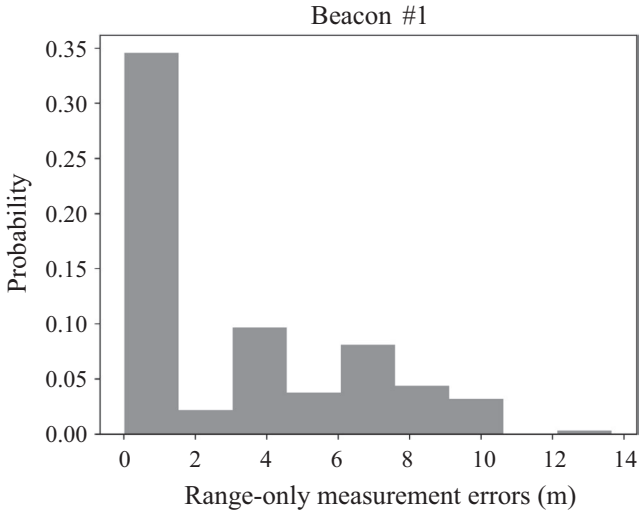

FIGURE 7 Measurement errors of the first beacon

Figure 6 shows range-only mapping results using the TOA data fusion and proposed method in the real indoor environment, and Table 5 shows mapping errors of three beacons. The locations of beacons #2 and #3 were accurately mapped using both methods, but the location of beacon #1 was inaccurately mapped by the TOA data fusion. Table 6 lists the mean measurement errors of the three beacons. The measurement error of a beacon is defined as the absolute difference between the observed (z) and ground truth measurements (z_{GT}). The mean measurement errors of beacons #2 and #3 were small. By contrast, the mean measurement error of beacon #1 was extremely large. Figure 7 shows the probability distribution of the measurement errors of beacon #1. The figure verifies that range-only measurements from beacon #1 were heavily affected by the propagation delays and blockage errors. Therefore, the TOA data fusion inaccurately estimated the location of beacon #1. In addition, the proposed method estimated the location of beacon #1 more accurately than did the TOA data fusion. Only the location uncertainty of beacon #1 was slightly larger than the location uncertainties of other beacons.

6 | CONCLUSION

This study proposed a robust range-only beacon mapping method in a multipath environment. The study showed that the proposed method estimated the locations of range-only beacons in a more robust fashion using the RANSAC-based feature initialization with the RoMA and the UKF-based feature update. The RANSAC-based feature initialization with the RoMA predicted the initial mean and covariance of the location of a range-only beacon, and it filtered out unreliable range-only measurements. The UKF-based feature updated the initially predicted mean and covariance of a range-only beacon using reliable range-only measurements. Moreover, the study showed that with the proposed method, the accurate locations of range-only beacons could be autonomously mapped even though a large portion of range-only measurements was affected by the multipath propagation. The location uncertainties of the range-only beacons were also estimated using the proposed method. The performance of the proposed method was verified through simulations using a realistic sensor model and through experiments in a real indoor environment.

ACKNOWLEDGMENTS

This work was supported by IITP grants (No. 2017-0-00067, 2017-0-00306). The authors thank Mr. M. Zaigham Zaheer for his constructive comments.

ORCID

Byungjae Park https://orcid.org/0000-0002-8952-0736

REFERENCES

1. Y. Gu, A. Lo, and I. Niemegeers, *A survey of indoor positioning systems for wireless personal networks*, IEEE Commun. Surv. Tutorial **11** (2009), no. 1, 13–32.
2. T.-H. Yi, H.-N. Li, and M. Gu, *Characterization and extraction of global positioning system multipath signals using an improved particle-filtering algorithm*, Meas. Sci. Technol. **22** (2011), no. 7, 075101:1–11.
3. P. Zandbergen, *Accuracy of iPhone locations: a comparison of assisted GPS, WiFi and Cellular Positioning*, Trans. GIS **13** (2009), no. 1, 5–25.
4. W. Chen and X. Sun, *Performance improvement of GPS single frequency, single epoch attitude determination with poor satellite visibility*, Meas. Sci. Technol. **27** (2016), no. 7, 075104:1–14.
5. H. Lui et al., *Survey of wireless indoor positioning techniques and systems*, IEEE Trans. Syst. Man Cybern. Part C **37** (2007), no. 6, 1067–1080.
6. A.H. Sayed, A. Tarighat, and N. Khajehnouri, *Network-based wireless location: challenges faced in developing techniques for accurate wireless location information*, IEEE Signal Process. Mag. **22** (2005), no. 4, 24–40.
7. K. Lee et al., *New TDOA based three dimensional positioning method for 3GPP LTE system*, ETRI J. **39** (2017), no. 2, 264–274.
8. T. Gigl et al., *Analysis of a UWB indoor positioning system based on received signal strength*, in Proc. Workshop Position. Navig. Commun., Hannover, Germany, Mar. 2007, pp. 97–101.
9. M. Kok, J.D. Hol, and T.B. Schon, *Indoor positioning using ultrawideband and inertial measurements*, IEEE Trans. Veh. Technol. **64** (2015), no. 4, 1293–1303.
10. http://www.ubisense.net.
11. N.A. Alsindi, B. Alavi, and K. Pahlavan, *Measurement and modeling of ultrawideband TOA-based ranging in indoor multipath environments*, IEEE Trans. Veh. Technol. **58** (2009), no. 3, 1046–1058.
12. Y. Luo and C.L. Law, *Indoor positioning using UWB-IR signals in the presence of dense multipath with path overlapping*, IEEE Trans. Wireless Commun. **11** (2012), no. 10, 3734–3743.

13. H.A.B.F. de Oliveira et al., *An efficient directed localization recursion protocol for wireless sensor networks*, IEEE Trans. Comput. **58** (2009), no. 5, 677–691.
14. A. Savvides, C.C. Han, and M.B. Strivastava, *Dynamic fine-grained localization in ad-hoc networks of sensors*, in Proc. ACM Ann. Int. Conf. Mobile Comput. Netw., Rome, Italy, 2001, pp. 166–179.
15. D.K. Goldenberg et al., *Localization in sparse networks using sweeps*, in Proc. ACM Ann. Int. Conf. Mobile Comput. Netw., Los Angeles, CA, USA, Sept. 2006, pp. 110–121.
16. X. Wang et al., *Component-based localization in sparse wireless networks*, IEEE/ACM Trans. Network. **19** (2011), no. 2, 540–548.
17. G. Kantor and S. Singh, *Preliminary results in range-only localization and mapping*, in Proc. IEEE Int. Conf. Robot. Autom., Washington, DC, USA, May 2002, pp. 1818–1823.
18. F. Caballero, L. Merino, and A. Ollero, *A general gaussian-mixture approach for range-only mapping using multiple hypotheses*, in Proc. IEEE Int. Conf. Robot. Autom., Anchorage, AK, USA, May 2010, pp. 4404–4409.
19. J.L. Blanco, J.A. Fernández-Madrigal, and J. González, *Efficient probabilistic range-only SLAM*, in Proc. IEEE/RSJ Int. Conf. Intell. Robot Syst., Nice, France, Sept. 2008, pp. 1017–1022.
20. E. Olson, J.J. Leonard, and S. Teller, *Robust range-only beacon localization*, IEEE J. Oceanic Eng. **31** (2006), no. 4, 949–958.
21. W.L. Chan, C.S. Lee, and F.B. Hsiao, *Real-time approaches to the estimation of local wind velocity for a fixed-wing unmanned air vehicle*, Meas. Sci. Technol. **22** (2011), no. 10, 105203.
22. S.J. Lee et al., *Feature map management for mobile robots in dynamic environments*, Robotica **28** (2010), no. 1, 97–106.
23. C. Kim, R. Sakthivel, and W.K. Chung, *Unscented FastSLAM: a robust and efficient solution to the SLAM problem*, IEEE Trans. Rob. **24** (2008), no. 4, 8080–8820.
24. J. González et al., *Mobile robot localization based on ultra-wideband ranging: a particle filter approach*, Robot. Auton. Syst. **57** (2009), no. 5, 496–507.
25. J. Martínez et al., *Mobile robot motion estimation by 2D scan matching with genetic and iterative closest point algorithms*, J. Field Robot. **23** (2006), no. 1, 21–34.

AUTHOR BIOGRAPHIES

Byungjae Park received his BS, MS, and PhD degrees in mechanical engineering from POSTECH in 2005, 2007, and 2013, respectively. He is currently a senior researcher at Electronics and Telecommunications Research Institute (ETRI). His main research interests are robotic perception, sensor fusion, mapping, and localization.

Sejin Lee received his BS degree in mechanical engineering from Hanyang University in 2003, and his MS and PhD degrees in mechanical engineering from POSTECH in 2005 and, 2009, respectively. From 2010 to 2013, he worked for the Department of Applied Robotics, Kyungil University. Since 2013, he has been with the Division of Mechanical and Automotive Engineering, Kongju National University, where he is now an associate professor. His main research interests are sensor fusion, simultaneous localization and mapping for mobile robot navigation, and deep learning.